HOKKAIDO UNIVERSITY

Title	Fluoride-target-assisted growth of Pb2OF2 oxyfluoride films with anion ordering and high dielectric constant
Author(s)	Muraki, Rion; Marunouchi, Ko; Zhou, Weikun et al.
Citation	Journal of materials chemistry C https://doi.org/10.1039/d5tc01975c
Issue Date	2025-09-16
Doc URL	https://hdl.handle.net/2115/98108
Type	journal article
File Information	Revised_Manuscript_final.pdf

Hokkaido University Collection of Scholarly and Academic Papers : HUSCAP

Fluoride-target-assisted growth of Pb_2OF_2 oxyfluoride films with anion ordering and high dielectric constant

Rion Muraki[1], Ko Marunouchi[1], Weikun Zhou[1], Akira Chikamatsu[2], Hiromichi Ohta[3], and Tsukasa Katayama[3]*

[1]Graduate School of Information Science and Technology, Hokkaido University, N14W9, Kita, Sapporo 060-0814, Japan

[2]Department of Chemistry, Faculty of Science, Ochanomizu University, 2-1-1 Otsuka, Bunkyo-ku, Tokyo 112-8610, Japan

[3]Research Institute for Electronic Science, Hokkaido University, N20W10, Kita, Sapporo 001-0020, Japan

E-mail: katayama@es.hokudai.ac.jp

Abstract

Recent research increasingly focuses on mixed-anion compounds, wherein oxygen sites in the metal oxides are substituted with other anions. However, the synthesis of such compounds remains limited compared to conventional oxides, highlighting the need for new fabrication methods. In this study, oxyfluoride Pb_2OF_2 films are synthesized using pulsed laser deposition (PLD) with a PbF_2 target. The substrate temperature plays a crucial role in stabilizing the oxyfluoride phase, with an optimal temperature of approximately 200 °C. Furthermore, (110)-oriented growth on perovskite-type single-crystal oxide substrates was achieved, wherein oxygen and fluorine ions exhibited out-of-plane ordering. The (110)-oriented Pb_2OF_2 films demonstrated a relatively high dielectric constant ($\varepsilon_r = 22$)– four times larger than that of the polycrystalline films– likely due to enhanced ionic response resulting from improved structural ordering.

1. Introduction

Metal oxides exhibit a wide range of functionalities, including ferroelectricity and high-temperature superconductivity [1,2]. Traditionally, these properties have been controlled by modifying the cation species or altering the crystal structure. However, in recent years, mixed-anion compounds—where some oxygen sites in metal oxides are substituted with other anions such as fluorine or nitrogen—have attracted significant attention [3−7]. For example, oxyfluorides have attracted attention as next-generation nonlinear optical materials for the deep ultraviolet and mid-infrared regions. They possess a broad transparency window, a large nonlinear optical coefficient, excellent phase-matching, and a high laser damage threshold [5]. This is because the incorporation of fluorine increases the probability of crystallizing a non-centrosymmetric structure, and fluorine's high electronegativity expands the transparency range and widens the bandgap [5]. Furthermore, due to the difference in valency between O^{2-} and F^{-} ions, the application of an electric field can displace oxygen and fluorine in opposite directions [7]. This has led to the discovery of new operating principles of antiferroelectricity, which differ from those found in oxides [7].

A common approach for synthesizing mixed-anion compounds involves mixing oxides with fluorides or nitrides, followed by heating to induce a reaction. For example, heating a mixture of PbO and PbF_2 at 200 °C yields Pb_2OF_2, in which oxygen and fluorine ions are ordered, with oxygen forming a one-dimensional arrangement [8−10].

In contrast to powder synthesis, the fabrication of mixed-anion compounds in thin-film form requires different approaches. Several methods have been reported. One such approach is topotactic fluorination, in which an oxide film is first fabricated and then reacted with a fluorine source to form an oxyfluoride [11−14]. For instance, reacting $SrFeO_x$ thin films with polyvinylidene fluoride at low temperatures yields perovskite $SrFeO_2F$ thin films [11,12]. Oxyfluoride films can also be directly synthesized. Direct synthesis offers advantages such as achieving a uniform chemical composition (fluorine content) along the depth of the film. One such method utilizes an oxyfluoride target to transfer

its composition to the film [15−17]. Another approach involves using a fluoride target, with oxygen introduced during film deposition to form the oxyfluoride [18]. For example, InOF films can be fabricated via pulsed laser deposition (PLD) using an InF_3 target, where the fluoride reacts with oxygen in the chamber [18]. Fluoride target-based synthesis enables broad control over the fluorine content, which could facilitate the discovery of new oxyfluoride phases. However, reports on the direct synthesis of oxyfluoride thin films using fluoride targets remain limited. Additionally, in thin film growth, strain from the substrate can be used to align the orientation of films, which has been reported to reduce defects and enhance functionality [19]. Therefore, comparing the synthesis and properties of polycrystalline and oriented oxyfluoride films is of great importance.

In this study, we synthesized Pb_2OF_2 oxyfluoride thin films using PLD with a PbF_2 fluoride target and investigated the effect of substrate temperature on phase formation and film crystallinity. Additionally, we achieved (110)-oriented growth of Pb_2OF_2, with out-of-plane ordering of oxygen and fluorine. The dielectric properties of the films were also evaluated, signifying that the (110)-oriented Pb_2OF_2 films exhibit a significantly higher dielectric constant (ε_r = 22) compared to their polycrystalline counterparts (ε_r = 5).

2. Experiment

$Pb(O,F)_x$ films were deposited using the PLD technique with a PbF_2 ceramic (Toshima Manufacturing Co., Ltd.) target. During deposition, the substrate temperature (T_s) was maintained between 40 °C and 300 °C, and the nitrogen pressure (P_{N2}) was set at 1×10^{-3} Torr. Two types of substrates were used: $TiN/SiO_2/Si$ substrates and 0.5 wt.%-Nb-doped $SrTiO_3(001)$ (Nb:STO) substrates. In the $TiN/SiO_2/Si$ substrates, the SiO_2 layer refers to a natural oxide film formed on the surface of the Si substrate. The TiN electrode layer was deposited by PLD using a TiN ceramic target at T_s = 600 °C and $P_{N2} = 1 \times 10^{-5}$ Torr.

The chemical composition of the films was analyzed by energy-dispersive X-ray spectroscopy

(EDS) attached to a scanning electron microscope (SEM, SU8230, Hitachi Co.), using an electron accelerating voltage of 5 keV. The crystal structures of the films were evaluated by X-ray diffraction (XRD, ATX-G, Rigaku Co.) with Cu $K\alpha_1$ radiation and grazing-incidence X-ray diffraction (GI-XRD) measurements were performed with an incident X-ray angle of 0.5°. Film thickness was determined through X-ray reflectivity (XRR) measurements. Dielectric properties were measured using an LCR meter (E4980, Keysight Co.) at 25 °C. For these measurements, Pt top electrodes with a diameter of 100 μm were applied, with either the TiN electrode layer or the Nb:STO substrate serving as the bottom electrode.

3. Results and discussion

3.1. Film deposition on TiN/SiO_2/Si substrates as a function of T_s

Figure 1(a) shows the EDS spectra of the films deposited on TiN/SiO_2/Si substrates at T_s = 40 °C and 200 °C. The spectra are normalized to the Pb M peak, and peaks corresponding to N Kα, O Kα, and F Kα are observed. The O Kα peak is also derived from the TiN/SiO_2/Si substrates, which contain oxygen ions due to the presence of the SiO_2 layer and their incorporation into the TiN lattice. The film deposited at T_s = 200 °C exhibits a lower F Kα peak and a higher O Kα peak compared to the film deposited at T_s = 40 °C.

Figure 1(b) presents the intensity ratio of the F Kα to Pb M peaks as a function of T_s. At T_s = 40 °C, the intensity ratio is 1.6— nearly identical to that of PbF_2 powder (indicated by dotted line in the figure)— suggesting successful transfer of target composition to the thin film. As T_s increases, the intensity ratio monotonically decreases to 0.9 at T_s = 200 °C. In contrast, at T_s > 250 °C, the F Kα peak disappears completely, and a diffraction peak corresponding to PbO appears at T_s = 300 °C. These results suggest that, even under a nitrogen atmosphere, residual oxygen in the chamber leads to the substitution of fluorine by oxygen at higher T_s. In our experiment, the base pressure of the vacuum chamber was approximately 1×10^{-7} Torr. At this pressure, residual gases such as water vapor and other

oxygen-containing species are still present, while fluorine is not included in the background and is supplied only from the target. At higher T_s, we speculate that the deposited films reacted with these residual oxygen species, resulting in the substitution of fluorine by oxygen.

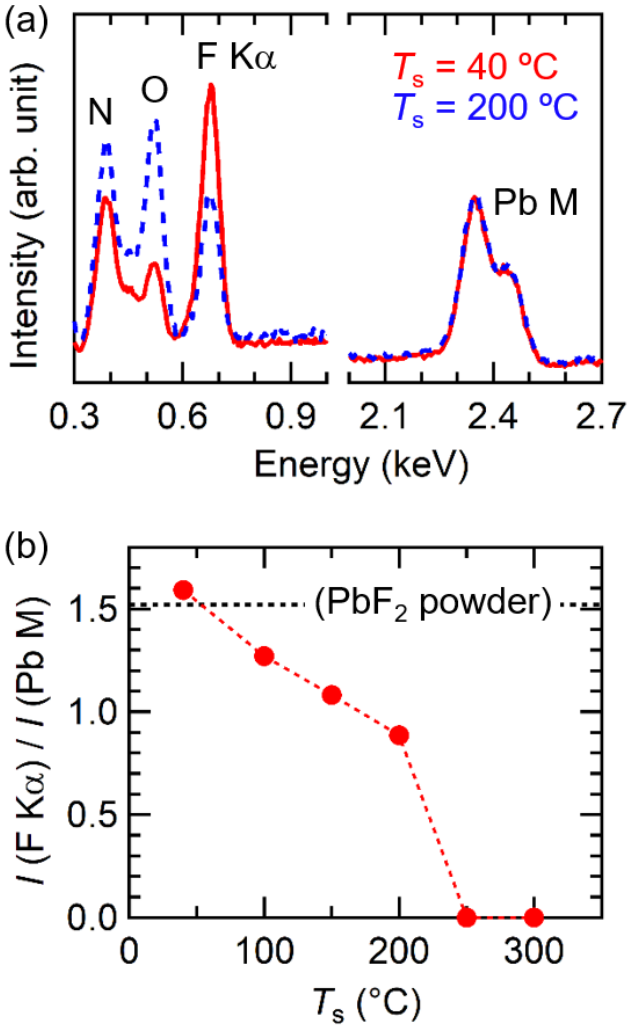


Figure 1. (a) EDS spectra of the films deposited on TiN/SiO_2/Si substrates at T_s = 40 °C and 200 °C. (b) The intensity ratio of the F Kα to the Pb M peaks for the films as a function of T_s.

Figure 2(a) shows the GI-XRD patterns of the films deposited at T_s = 40, 100, 150, and 200 °C. The thickness of the films was 40 nm. At T_s = 40 °C, the 111 diffraction peak of PbF_2 appears at 2θ = 26°, along with the 220 peak. The calculated a-axis length of the film (5.94 Å) matches the lattice

constant of bulk PbF_2 (cubic structure, a = 5.940 Å [20], Fig. 2(b)), confirming the presence of PbF_2 in the film deposited at T_s = 40 °C. With increasing T_s, new diffraction peaks corresponding to the Pb_2OF_2 phase (Fig. 2(c)) emerge. In particular, at T_s = 200 °C, the PbF_2 peaks significantly weaken, and distinct peaks corresponding to Pb_2OF_2, such as the 110, 021, 220, and 222 peaks, become prominent. The calculated a- and c-axis lengths of the film are 8.12 Å and 5.73 Å, respectively, closely aligning with those of bulk Pb_2OF_2 (tetragonal structure, a = 8.157 Å, c = 5.723 Å [8]). At T_s = 250 °C, fluorine is completely removed (Fig. 1(b)), and consequently, no XRD diffraction peaks were detected. According to the Scherrer equation, the crystalline size of the Pb_2OF_2 phase in the film deposited at T_s = 200 °C, estimated from the diffraction peak, is 13 nm.

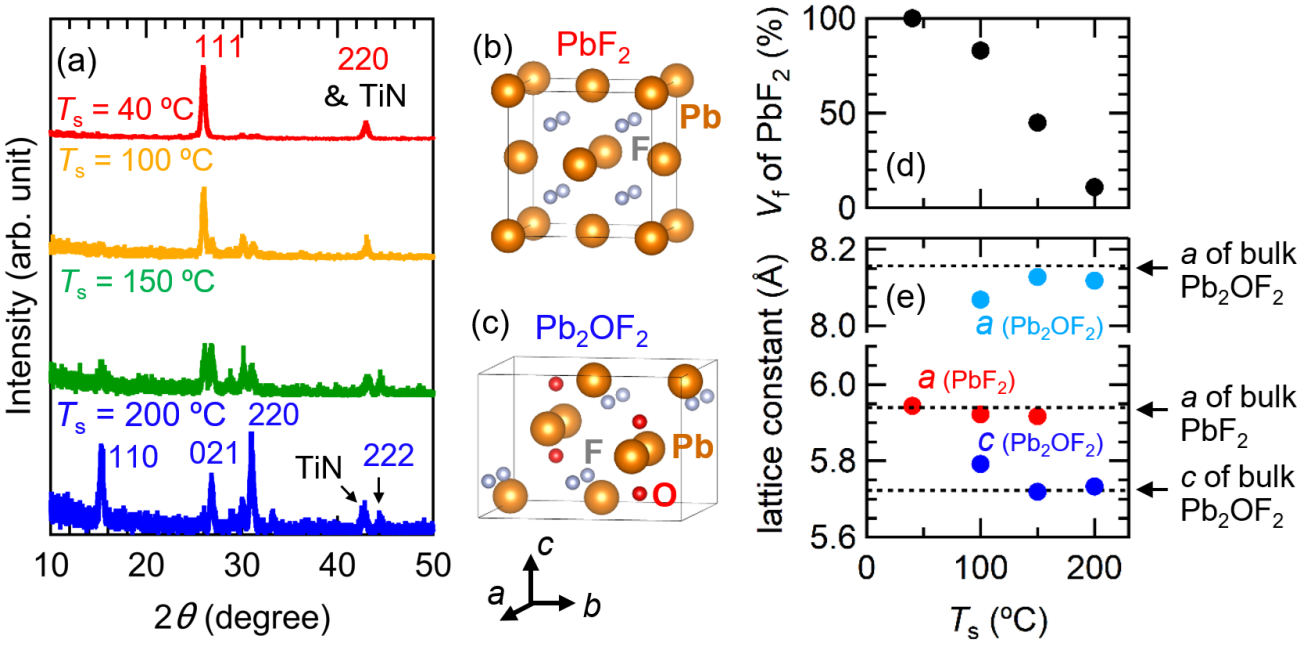


Figure 2. (a) GI-XRD patterns of the films deposited on $TiN/SiO_2/Si$ substrates as a function of T_s. Crystal structures of (b) PbF_2 and (c) Pb_2OF_2. (d) Volume fraction (V_f) of PbF_2 and (e) lattice constants of PbF_2 and Pb_2OF_2 phases in the films as a function of T_s.

Figure 2(d) illustrates the volume fraction (V_f) of PbF_2 as a function of T_s. The V_f was calculated from the peak intensity ratio of the PbF_2 111 peak to the Pb_2OF_2 021 peak (Fig. S1). With increasing

T_s, the V_f value of PbF_2 decreases monotonically, consistent with the EDS results, indicating the progressive decrease in fluorine content with rising T_s. Figure 2(e) presents the lattice constants of the PbF_2 and Pb_2OF_2 phases in the films as a function of T_s. The lattice constants are nearly identical to those of the bulk materials; however, they exhibit slight variations with T_s. These findings suggest that the compositions of the phases were to those of their bulk counterparts, although minor differences existed in the anion ratio.

3.2. (110)-oriented growth on Nb:STO(001) substrate

Pb_2OF_2 films were also fabricated on Nb:STO(001) single-crystal substrates. Figure 3(a) shows the out-of-plane $2\theta-\theta$ XRD pattern of the film with a thickness of 40 nm. At T_s = 200 °C, a diffraction peak corresponding to PbO was observed; therefore, results for the film deposited at T_s = 175 °C are presented. The 110, 220, 330, and 440 diffraction peaks of Pb_2OF_2 were detected, confirming that the Pb_2OF_2 phase is oriented along the [110] direction. This indicates that O^{2-} and F^- ions are ordered along the out-of-plane direction, as illustrated in Fig. 4(a). Although a PbF_2 impurity phase was also observed, the corresponding V_f, calculated from the two-dimensional 2θ–χ scans, was relatively low (7%).

PbF_2 has a CaF_2-type structure, in which Pb atoms occupy the face-centered cubic (fcc) lattice positions. In such a structure, the 001 diffraction peak is forbidden due to symmetry. Pb_2OF_2 has a similar Pb sublattice arrangement, where the [001] direction of PbF_2 corresponds to the [110] direction of Pb_2OF_2. As shown in the Fig. 3(a), diffraction peaks from PbF_2 such as 002 and 004 appear near the 220 and 440 peaks of Pb_2OF_2, indicating a structural similarity between the two phases. However, near the 110 peak of Pb_2OF_2, no corresponding PbF_2 peak is observed. This 110 peak of Pb_2OF_2 can be regarded as a kind of superlattice reflection arising from periodic lattice distortions caused by the ordering of O^{2-} and F^- ions.

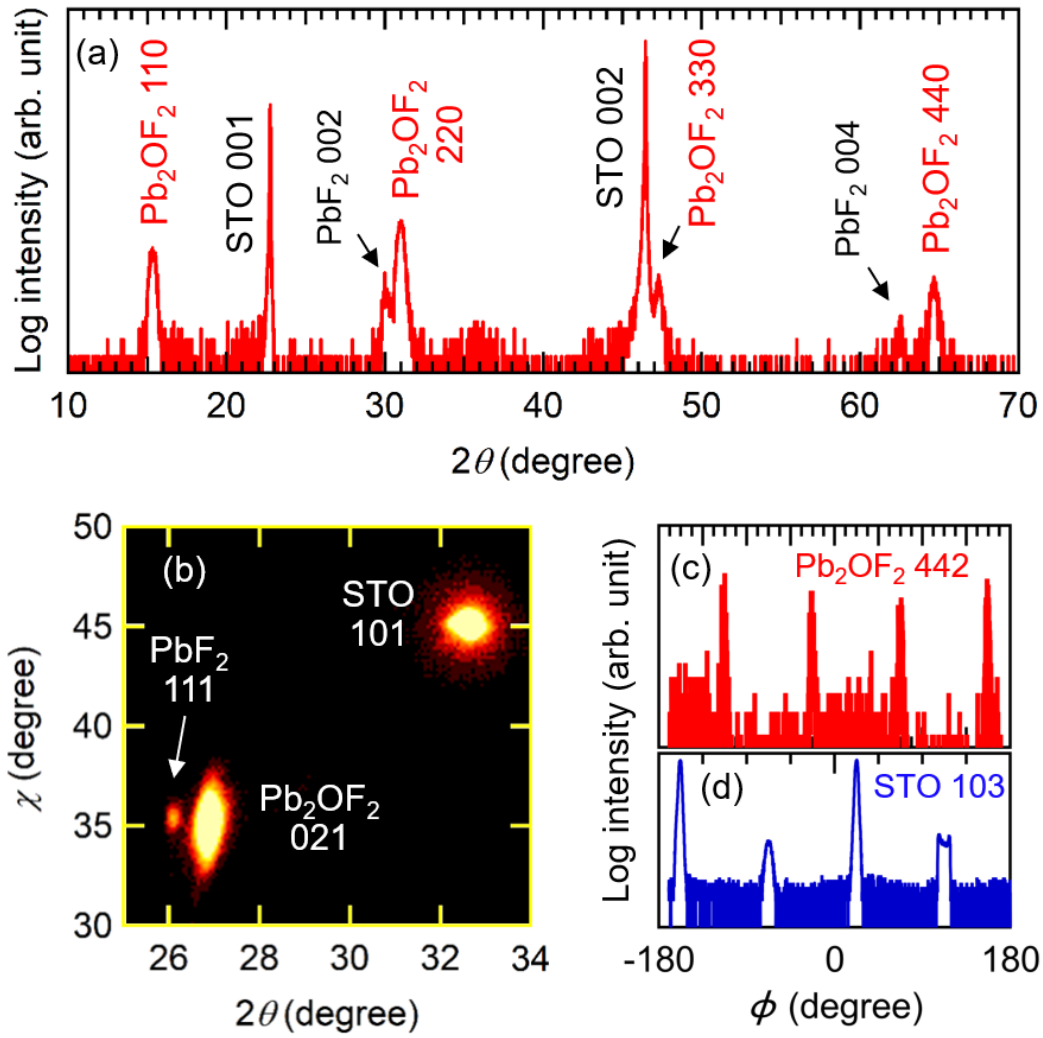


Figure 3. (a) Out-of-plane 2θ–θ XRD pattern, (b) two-dimensional 2θ–χ scan around the STO 110 diffraction peak, and ϕ-scan of the (c) Pb_2OF_2 442 and (d) $SrTiO_3$ 103 diffraction peaks for the Pb_2OF_2 film deposited on Nb:STO(001) substrate.

To investigate the in-plane relationship between the film and the substrate, two-dimensional 2θ–χ scans were performed. The Pb_2OF_2 021 diffraction peak was observed near the STO 101 diffraction peak (Fig. 3(b)), and the Pb_2OF_2 202 diffraction peak appeared near the STO 111 diffraction peak (Fig. S2). Additionally, ϕ-scan measurements show that the Pb_2OF_2 442 diffraction peak appeared with fourfold symmetry, with ϕ-values shifted by 45° relative to those of the STO 103 diffraction peak (Fig. 3(c,d)). These results indicate that the [1-10] direction of Pb_2OF_2 ($[1\text{-}10]_{Pb2OF2}$) is nearly parallel

to the [110] direction of the Nb:STO substrate ($[110]_{STO}$). Figure 4(b) shows a plan-view image of the crystal structure of Pb_2OF_2 and STO. The Pb positions in Pb_2OF_2 closely correspond to the Sr and Ti positions in STO. The lattice mismatch is only 4%, and this good lattice matching facilitates the (110)-oriented growth of the film. The lattice constants of the film are a = 8.140 Å and c = 5.79 Å, similar to those of the bulk material [8].

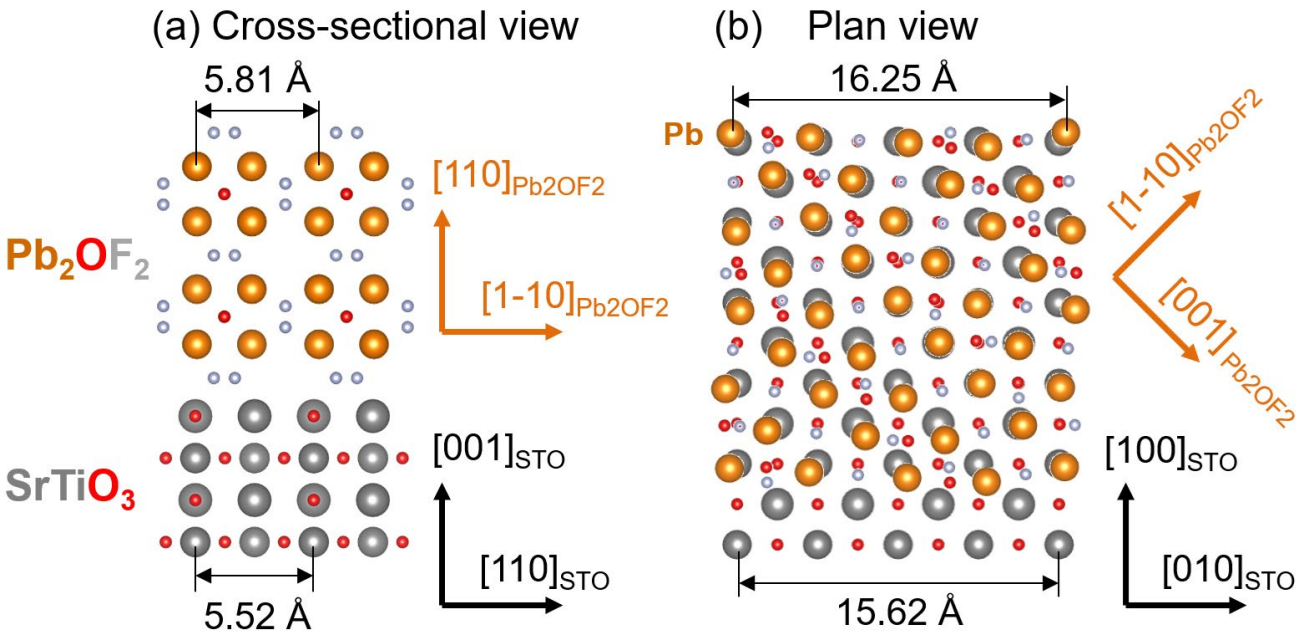


Figure 4. (a) Cross-sectional and (b) plan-view images of the crystal structures of (110)-oriented Pb_2OF_2 film and Nb:STO(001) substrate.

3.3. Dielectric properties of the films

Figure 5(a, b) shows the relative dielectric constant (ε_r) and dielectric loss (tanδ) of PbF_2 and Pb_2OF_2 polycrystalline films deposited on TiN/SiO_2/Si substrates (at T_s of 40 °C and 200 °C, respectively). and a (110)-oriented Pb_2OF_2 film grown on an Nb:STO substrate at T_s = 175 °C. The films were 40 nm thick. The tanδ values remain below 0.1, confirming the insulating nature of the films. This observation aligns with earlier reports indicating that bulk PbF_2 and Pb_2OF_2 exhibit

insulating properties, with bandgaps of 5.7 eV and 3.8 eV, respectively [8,21].

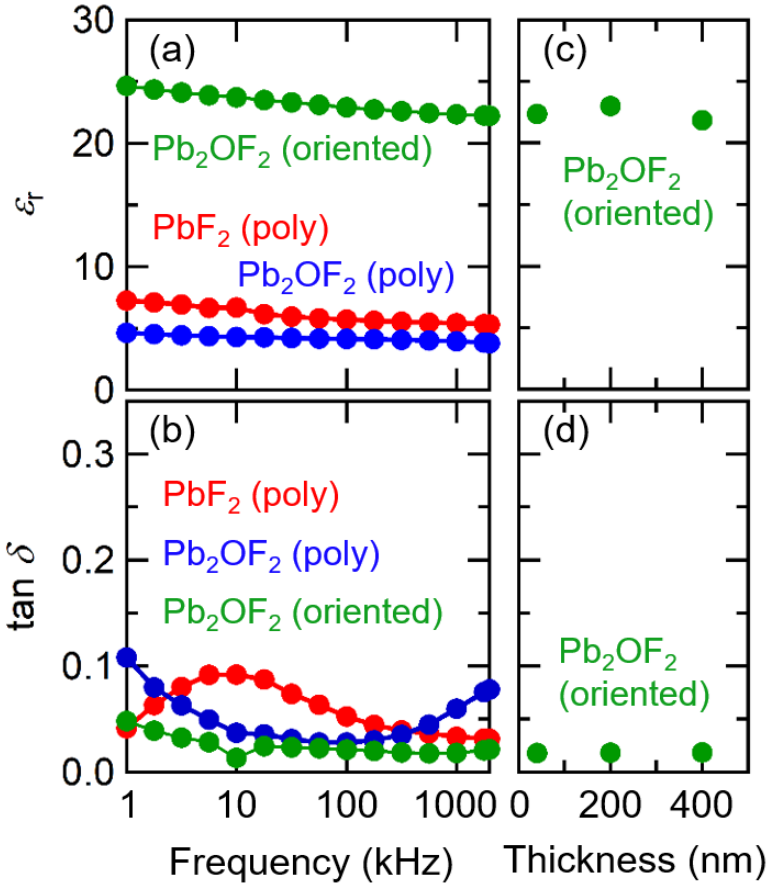


Figure 5. (a) ε_r and (b) tanδ of the PbF_2 and Pb_2OF_2 polycrystal films deposited on TiN/SiO_2/Si substrates and (110)-oriented Pb_2OF_2 film deposited on Nb:STO substrate. (c) ε_r and (d) tanδ of (110)-oriented Pb_2OF_2 films at 1000 kHz as a function of thickness.

The tanδ value of the (110)-oriented Pb_2OF_2 film is lower than that of the polycrystalline film due to the reduced grain boundary density, which typically contribute to leakage currents. In addition, SEM measurements reveal that the surface of the polycrystalline Pb_2OF_2 film is significantly rougher than that of the (110)-oriented film, which also serves as a source of leakage current. Furthermore, the ε_r value of the (110)-oriented Pb_2OF_2 film is approximately 22, about four times higher than that of the polycrystalline film. To verify this, we varied the thickness of the (110)-oriented Pb_2OF_2 films from 40 to 200 nm (Figs. 5(c, d), S4), and the ε_r value remained consistent, confirming its reliability. As per

reports, in PbF_2, ε_r is influenced by both the polarization of the electron cloud under an applied voltage and the ionic conductivity of fluorine ions [22]. The higher ε_r observed in the (110)-oriented Pb_2OF_2 film, compared to the polycrystalline film, is likely due to the reduced grain boundary density and the ordered alignment of oxygen and fluorine ions along the out-of-plane direction, possibly enhancing the ionic response to the applied electric field.

4. Conclusion

Oxyfluoride Pb_2OF_2 films were directly fabricated using PLD with a PbF_2 target. The substrate temperature played a crucial role in the stabilization of the oxyfluoride phase. Additionally, the (110)-oriented growth of the oxyfluoride phase was achieved, wherein oxygen and fluorine ions exhibit out-of-plane ordering. Dielectric property measurements revealed that the (110)-oriented Pb_2OF_2 films exhibit a relatively high ε_r value, about four times larger than that of the polycrystalline films, attributed to the reduced grain boundary density and an improved ionic response due to the ordered oxygen and fluorine alignment. These results demonstrate the feasibility of direct synthesis of oxyfluoride thin films using fluoride targets and highlight their potential for dielectric applications.

Supporting information

Detailed XRD results are provided in the Supporting Information.

Acknowledgments

This work was supported by JST PRESTO (JPMJPR21Q3) and JST A-STEP (JPMJTR24032140).

References

[1] N. Setter, D. Damjanovic, L. Eng, G. Fox, S. Gevorgian, S. Hong, A. Kingon, H. Kohlstedt, N.

Y. Park, G. B. Stephenson, I. Stolitchnov, A. K. Taganstev, D. V. Taylor, T. Yamada, and S. Streiffer, Ferroelectric thin films: Review of materials, properties, and applications. *J. Appl. Phys.* **100**, 051606 (2006).

[2] B. Keimer, S. A. Kivelson, M. R. Norman, S. Uchida, and J. Zaanen, From quantum matter to high-temperature superconductivity in copper oxides. *Nature* **518**, 179–186 (2015).

[3] H. Kageyama, K. Hayashi, K. Maeda, J. P. Attfield, Z. Hiroi, J. M. Rondinelli, and K. R. Poeppelmeier, Expanding frontiers in materials chemistry and physics with multiple anions. *Nat Commun* **9**, 772 (2018).

[4] K. Maeda, F. Takeiri, G. Kobayashi, S. Matsuishi, H. Ogino, S. Ida, T. Mori, Y. Uchimoto, S. Tanabe, T. Hasegawa, N. Imanaka, and H. Kageyama, Recent Progress on Mixed-Anion Materials for Energy Applications, *Bull. Chem. Soc. Jpn* **95**, 1, 26–37 (2022).

[5] S. Bai, D. Wang, H. Liua, and Y. Wang, Recent advances of oxyfluorides for nonlinear optical applications. *Inorg. Chem. Front.* **8**, 1637 (2021).

[6] M. Ahmed, and G. Xinxin, A review of metal oxynitrides for photocatalysis. *Inorg. Chem. Front*. **3**, 578-590 (2016).

[7] T. Katayama, A. Chikamatsu, and M. Hirayama, Antiferroelectric behavior in mixed-anion $Bi_2TiO_4F_2$ induced by rotation of TiO_3F_3 octahedra. *Adv. Funct. Mater.* **2500489**, 1, (2025).

[8] Y. Inaguma, K. Ueda, T. Katsumata, Y. Noda, Low-temperature formation of Pb_2OF_2 with O/F anion ordering by solid state reaction. *J. Solid State Chem.* **277**, 363-367 (2019).

[9] B. Aurivillius, X-ray studies of lead oxide fluoride and related compounds. *Chem. Scripta* **10**, 156–158 (1976).

[10] C. Follet-Houttemane, J. C. Boivin, D. J. Thomas, J. C. Champarnaud-Mesjard, D. Mercurio, B. Frit, Thermal dependence of conduction properties in the Bi_2O_3 Pb_2OF_2 system. *Solid State Ionics* **23**, 173-178 (1987).

[11] E. J. Moon, Y. Xie, E. D. Laird, D. J. Keavney, C. Y. Li, S. J. May, Fluorination of epitaxial

oxides: synthesis of perovskite oxyfluoride thin films. *J. Am. Chem. Soc.* **136**, 6, 2224–2227 (2014).

[12] T. Katayama, A. Chikamatsu, Y. Hirose, R. Takagi, H. Kamisaka, T. Fukumura, and T. Hasegawa, Topotactic fluorination of strontium iron oxide thin films using polyvinylidene fluoride. *J. Mater. Chem. C* **2**, 5350−5356 (2014).

[13] T. Onozuka, A. Chikamatsu, T. Katayama, Y. Hirose, I. Harayama, D. Sekiba, E. Ikenaga, M. Minohara, H. Kumigashira, and T. Hasegawa, T. Reversible changes in resistance of perovskite nickelate $NdNiO_3$ thin films induced by fluorine substitution. *ACS Appl. Mater. Interfaces* **9**, 10882−10887 (2017).

[14] T. Nishimura, T. Katayama, S. Mo, A. Chikamatsu, and T. Hasegawa, Improvement of electric insulation in dielectric layered perovskite nickelate films via fluorination. *J. Mater. Chem. C* **10**, 1711−1717 (2022).

[15] H. Kim, R. C. Y. Auyeung, A. Piqué, Transparent conducting F-doped SnO_2 thin films grown by pulsed laser deposition. *Thin Solid Films* **516**, 5052-5056 (2008).

[16] A. A. Yadav, E. U. Masumdar, A. V. Moholkar, M. Neumann-Spallart, K. Y. Rajpure, C. H. Bhosale, Electrical, structural and optical properties of SnO_2:F thin films: Effect of the substrate temperature. J. Alloys and Compounds **488**, 350-355 (2009).

[17] B. Xu, J. Hao, Q. Guo, J. Wang, G. Bai, B. Fei, S. Zhou, and J. Qiu, Ultrabroadband near-infrared luminescence and efficient energy transfer in Bi and Bi/Ho co-doped thin films. *J. Mater. Chem. C* **2**, 2482-2487 (2014).

[18] S. Okazaki, Y. Hirose, S. Nakao, C. Yang, I. Harayama, D. Sekiba, and T. Hasegawa, Epitaxial growth of indium oxyfluoride thin films by reactive pulsed laser deposition: Structural change induced by fluorine insertion into vacancy sites in bixbyite structure. *Thin Solid Films* **559**, 96-99 (2014)

[19] I. Fina, and F. Sánchez, Epitaxial Ferroelectric HfO_2 Films: Growth, Properties, and Devices.

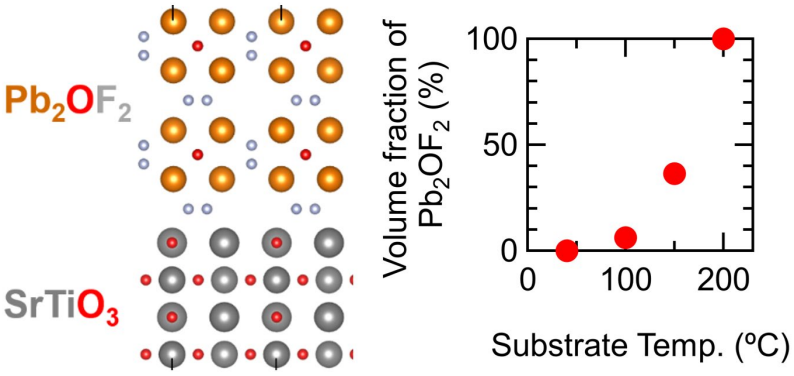
ACS Appl. Electron. Mater. 3, 4, 1530–1549 (2021).

[20] C. Erk, L. Hammerschmidt, D. Andrae, B. Paulus, and S. Schlecht, Low-temperature formation of cubic β-PbF_2: precursor-based synthesis and first-principles phase stability study. *Phys. Chem. Chem. Phys.* **13**, 6029-6035 (2011).

[21] J. H. Beaumont, A. J. Bourdillont, and J. Bordas, Optical properties of PbI_2 and PbF_2. *J. Phys. C: Solid State Phys.* **10** 761 (1977).

[22] G. A. Samara, Temperature and pressure dependences of the dielectric properties of PbF_2 and the alkaline-earth fluorides. *Phys. Rev. B* **13**, 4529 (1976).

Table of Contents



Fabrication methods for mixed-anion compounds are presented through the synthesis of lead oxyfluoride films. The work shows that controlling substrate temperature enables oriented growth, which enhances the material's dielectric constant.